RSC Advances

PAPER

View Article Online
View Journal | View Issue

Cite this: *RSC Adv.*, 2021, **11**, 14347

Fluorescence characteristics of dissolved organic matter during anaerobic digestion of oil crop straw inoculated with rumen liquid†

Lianghu Su,[a] Mei Chen,[a] Saier Wang,[a] Rongting Ji,[a] Chenwei Liu,[a] Xueqin Lu,[bc] Guangyin Zhen *[bde] and Longjiang Zhang*[a]

Fluorescence excitation–emission matrix (EEM) spectroscopy is a powerful tool for characterizing dissolved organic matter (DOM), a key component of anaerobic digestion. In this study, the fluorescence characteristics of DOM during 55 days of anaerobic digestion of oil crop straw inoculated with rumen liquid were investigated. EEM spectroscopy coupled with parallel factor analysis (PARAFAC) showed that three major fluorescence components, tyrosine- (C_1), humic- (C_2) and tryptophan-like substances (C_3), were identified in all DOM samples. The F_{max} values of C_1 and C_3 increased rapidly during the first 5 d, decreased dramatically from day 5 to day 35, and then remained stable, while C_2 was not biodegraded. The changes in the F_{max} values of the fluorescence components reflected the biodegradation of lignin and/or embedded cellulose by rumen microorganisms. The changes in the Stokes shift of the fluorescence peak were readily explained by the variation in the hydrophobic/hydrophilic fraction distribution. The humidification index (HIX) and A : T ratio of the DOM decreased after 5 d and then increased gradually. Compared with the McKnight fluorescence index (MFI), the Y fluorescence index (YFI) was better able to track the evolution of the DOM. Correlation analysis of the different fluorescence indices (intensities) and absorbance indices was also carried out. The EEM-PARAFAC individual components, HIX and A : T ratio were conveniently used to characterize the degree of anaerobic conversion of the organic matter, and the peak at the Stokes shift of ~1.0 μm^{-1} was used as one of the indicators showing the stabilization of anaerobic digestion. These findings may assist in developing fluorescence technology for monitoring the anaerobic digestion of crop straw.

Received 12th February 2021
Accepted 6th April 2021

DOI: 10.1039/d1ra01176f

rsc.li/rsc-advances

Introduction

Renewable energy sources (especially biomass) have been undergoing rapid development in recent years. It is predicted that biomass alone will account for two-thirds of directly used renewable energy in 2050.[1] Among the different forms of biomass, lignocellulosic materials, particularly crop straws, are an attractive source. China is the world's largest crop residue producer, and produced 897 Mt in 2016.[2] Anaerobic digestion offers a promising avenue for simultaneous recovery of biogas (also reducing greenhouse gas emissions), as a versatile renewable energy source, and of residual solids or liquid, as green fertilizers by means of the conversion of the organic matter in crop straw.[3]

In the anaerobic digestion process, dissolved organic matter (DOM) is the key component as a result of metabolism by microorganisms occurring in the water-soluble phase.[4,5] DOM is composed of the dissolved components of the organic matter input and the intermediates of microbial processes, and is considered as the directly assimilable carbon source for microorganisms compared with particulate organic matter.[5,6] Accordingly, the characterization of DOM is critical for understanding the degradation process of crop straw during anaerobic digestion.

Fluorescence excitation–emission matrix (EEM) spectroscopy is a powerful technique for characterizing DOM.[7,8] Fluorescence fingerprinting information, including peak intensity, peak location and distribution, spectra decomposition (including parallel factor analysis (PARAFAC), principal component analysis (PCA) and parallel factor framework-clustering analysis (PFFCA)) and energy-related information (including Stokes shift and the energy level of excited state) have

[a]*Nanjing Institute of Environmental Sciences, Ministry of Ecology and Environment, 8 Jiangwangmiao Street, Nanjing 210042, P. R. China. E-mail: zlj@nies.org*

[b]*Shanghai Key Lab for Urban Ecological Processes and Eco-Restoration, School of Ecological and Environmental Sciences, East China Normal University, Dongchuan Rd 500, Shanghai 200241, P. R. China. E-mail: gyzhen@des.ecnu.edu.cn*

[c]*Institute of Eco-Chongming (IEC), 3663 N. Zhongshan Rd, Shanghai 200062, P. R. China*

[d]*Shanghai Institute of Pollution Control and Ecological Security, 1515 North Zhongshan Rd (no. 2), Shanghai 200092, P. R. China*

[e]*Technology Innovation Center for Land Spatial Eco-restoration in Metropolitan Area, Ministry of Natural Resources, 3663 N. Zhongshan Road, Shanghai, 200062, P. R. China*

† Electronic supplementary information (ESI) available. See DOI: 10.1039/d1ra01176f

all been used for DOM characterization under different scenarios. Jaffe *et al.*[9] showed that changes in DOM composition could not be simply predicted from the DOM concentration.[10] Li *et al.*[4] investigated the chemical and structural changes in the DOM of dewatered sewage sludge and determined the degree of degradation of anaerobic digestion by a combination of EEM spectra and PARAFAC analysis (EEM-PARAFAC). Komatsu *et al.*[11] characterized the DOM fluorescence in wastewater during aerobic, anaerobic and anoxic treatment processes. Provenzano *et al.*[12] investigated the structural complexity and fluorescence intensity of the EEM contour maps of digestate derived from maize silage. Fluorescence EEM was also applied as a sensitive and efficient tool for assessing the dynamic changes and humification process of composting.[13,14] With regard to energy-related information, Xiao *et al.*[15–17] reported that the Stokes shift reflected the molecular weight and hydrophobicity of the DOM in membrane bioreactors.

To the best of our knowledge, few studies have focused on the fluorescence characteristics (especially energy-related information) of DOM during crop straw anaerobic biodegradation. In this study, the anaerobic digestion of the three main types of oil crop straw harvested in China, namely, peanut, soybean and oilseed rape, over a period of 55 days was investigated. Rumen microorganisms, found mainly in the specific stomachs of ruminant animals,[18] comprising a complex anaerobic microbial consortium, were adopted as the inoculum due to their ability to degrade the rigid three-dimensional matrix (cross-linking in cellulose, hemicellulose and lignin) of crop straw.[19] The anaerobic bioconversion performance of oil crop straw with rumen microorganisms was characterized by determining the quantities of volatile fatty acids (VFAs) and methane produced. EEM-PARAFAC was applied in order to analyse the composition and changes in the fluorescence components during the anaerobic digestion process. The changes in Stokes shift and fluorescence and absorbance indices (humification index, A : T ratio, McKnight fluorescence index (MFI), Y fluorescence index (YFI), E_2/E_3, spectral slope ratio) during anaerobic digestion were analysed in order to further unravel the fluorescence characteristics of biodegradation and the metabolic processes involved. Correlation analysis of the different fluorescence (intensities) and absorbance indices was also carried out.

Materials and methods

Oil crop straw and rumen liquid

Peanut (*Arachis hypogaea* L.), soybean (*Glycine max* L.) and oilseed rape (*Brassica napus* L.) are the main oil crops grown in China. Samples of these three types of oil crop straw were collected from Jiangsu Province, China. Following shredding, the different types of air-dried straw were sieved through a 40-mesh. The physicochemical properties of the three types of oil crop straw are listed in Table 1. The holocellulose (cellulose + hemicellulose) contents of oilseed rape, peanut and soybean straw were 54.67%, 44.31% and 58.89%, respectively. Compared with oilseed rape and peanut straw, soybean straw had a higher content of lignin (14.41%). The oil crop residue was further pulverized to 100-mesh using a planetary ball mill (TJ-2L, Tianjin Dongfang Tianjing Technology Development Co., Ltd, China) before anaerobic digestion.

Rumen contents were obtained from two dairy cattle freshly slaughtered at a local abattoir in Nanjing City, Jiangsu Province. The ruminal contents were squeezed through three layers of gauze to obtain the rumen fluid, which was transferred to the laboratory to provide the seed microorganisms. The pH of the rumen fluid was 6.87. A high-throughput sequencing technique was used for analysis of the community structure of the rumen bacterial microbiota, using the universal primers 338F (5′-ACT CCT ACG GGA GGC AGC AG-3′) and 806R (5′-GGACTA CHV GGG TWT CTA AT-3′). Seventeen bacterial phyla were represented in the rumen liquid (see Fig. S1 of the ESI†), with Firmicutes, Bacteroidetes and Proteobacteria being the most abundant phyla and accounting for 41.41%, 34.50% and 12.07% of the total bacterial sequences, respectively. Approximately 60% of the Firmicutes sequences were assigned to the class Clostridia, with the rest belonging to the classes Negativicutes, Bacilli, Erysipelotrichia and Unclassified Firmicutes. Within the class Clostridia, Lachnospiraceae and Ruminococcaceae were the largest families, accounting for 32.48% and 36.63%, respectively. The predominant genera included *Butyrivibrio* (4.69%), *Stomatobaculum* (7.23%) and *Ethanoligenens* (4.75%). As for the phylum Bacteroidetes, 57.73% of these sequences were assigned to the class Bacteroidia, and the rest to the classes Sphingobacteria (0.17%), Flavobacteriia (0.41%) and unclassified Bacteroidetes (41.69%). The Bacteroidetes sequences were assigned to nine genera, of which *Prevotella* was the main genus (49.8%). *Comamonas* was the largest genus (52.88%) of the Betaproteobacteria sequences. All of the archaeal sequences belonged to the genus *Methanobrevibacter*.

Experimental procedure

Anaerobic digestion of oil crop straw was carried out in reactors with a working volume of 500 mL. The media used contained the following ingredients (per litre):[20] 8 g $NaHCO_3$, 1 g KH_2PO_4, 3 g K_2HPO_4, 0.18 g NH_4Cl, 0.08 g $MgCl_2 \cdot 6H_2O$ and 0.03 g

Table 1 Physicochemical characteristics of three types of oil crop straw (%)

Type	Moisture content	Cellulose[a]	Hemicellulose[a]	Lignin[a]	Ash[a]
Peanut	10.62 ± 0.02	39.31	5.00	11.69	16.43 ± 0.35
Soybean	8.78 ± 0.00	43.79	15.1	14.41	4.32 ± 0.06
Oilseed rape	9.32 ± 0.00	42.47	12.2	10.43	12.59 ± 0.03

[a] Dry matter. The cellulose, hemicellulose, and lignin were analysed using an ANKOM 2000I Automated Fiber Analyzer (ANKOM Technology Corporation, Macedon, NY, USA).

$CaCl_2 \cdot 2H_2O$. A substrate of 10 g-VS L^{-1} (320 mL) was used in each test, while 80 mL of rumen fluid was used as the inoculum. Calcium carbonate was added as a buffer to maintain the pH above 6. Each reactor was connected to a mechanical agitator to gently mix (100 rpm) the contents, and the gas produced was measured by the automatic online analysis system. The digestion lasted for 55 d at 39 ± 0.5 °C.

Method of analysis

For the EEM analysis, all samples were filtered through a 0.45 μm membrane and diluted 20 times with ultrapure water (18 MΩ cm) due to their high fluorescence intensity. The fluorescence EEM were measured in a 1 cm quartz cuvette using an Aqualog fluorescence spectrometer (HORIBA Instruments Inc., Irvine, CA, USA) at 3 nm excitation wavelength intervals between 240 and 600 nm and emission wavelength coverage between 211 and 618 nm with 3.54 nm increments. The Aqualog fluorescence spectrometer contained an aberration-corrected double-grating excitation monochromator and an emission detector comprising a spectrograph with a thermoelectrically cooled back-illuminated CCD. The Aqualog spectrometer enabled simultaneous fluorescence and absorbance measurements to be made, with matching optical bandpass resolution, thus avoiding variations, and facilitated spectral correction of inner-filter effects (IFEs). The accompanying Aqualog-coupled software was equipped with a built-in tool for normalization of water Raman scattering as well as correction of the IFE and Rayleigh masking effects.[21] The intensities were further converted to Raman units (RU) by dividing the measured intensities by the Raman peak intensity of ultrapure water at Ex 350 nm. The fully corrected EEM data (the final dimensions of the data array were: 40 samples × 125 excitations × 121 emissions) were further analysed using PARAFAC with the Solo + MIA 8.6.1 software package from Eigenvector Research, Inc (Manson, WA, USA). A non-negativity constraint was applied to the parameters since negative concentrations and fluorescence intensities are chemically impossible.[22]

The Stokes shift is calculated as the difference between the excitation and emission frequencies according to Xiao *et al.*,[16,17] defined as:

$$\text{Stokes shift} = 1/\lambda_{Ex} - 1/\lambda_{Em} \quad (1)$$

where λ_{Ex} and λ_{Em} are the excitation and emission wavelengths (nm), respectively. By mapping the contour of the Stokes shift (see Fig. S2 of the ESI†) onto the actual EEM spectra of the DOM samples, the fluorescence intensity at each Stokes shift could be calculated from the EEM spectrum. Different fluorescence and absorbance indices (*i.e.* humification index, A : T ratio, MFI, YFI, E_2/E_3 and spectral slope ratio) were calculated from each corrected EEM. The humification index (HIX) was calculated from the ratio H/L, where H is the fluorescence intensity recorded at Ex 255 nm for the Em spectrum between 435 and 480 nm and *L* is the fluorescence intensity recorded at Ex 255 nm for the Em spectrum between 300 and 345 nm.[23] The A : T ratio is the ratio between the humic- and tryptophan-like fluorescence intensities, calculated from the ratio of the peak A (Ex 260/Em 450) and peak T (Ex 275/Em 304) intensities.[24] The MFI is the ratio of Ex/Em 370/450 nm to Ex/Em 370/500 nm.[25] The YFI is the ratio of the average fluorescence intensities in the range 350–400 over 400–450 nm with excitation at Ex 280 nm.[26] E_2/E_3 is the ratio of the absorption intensities at 250 and 365 nm.[27] The spectral slope ratio (S_R) is the ratio of the slope of the shorter wavelength region to that of the longer wavelength region, where wavelength intervals of 275–295 and 350–400 nm were used.[27]

For analysis of the VFAs, all samples were acidified with dilute sulfuric acid, centrifuged for 10 min at 10 000 rpm and filtered through 0.45 μm filters. The concentrations of the VFAs (acetic, propionic, isobutyric, *n*-butyric, isovaleric and *n*-valeric acids) were determined by gas chromatography (Shimadzu GC-2014, Kyoto, Japan) equipped with a flame ionization detector (FID) and analytical column Stabilwax-DA (30 m × φ 0.53 mm × δ 0.25 μm). The temperatures of the injector and FID were 150° and 240 °C, respectively.

Results and discussion

Performance of anaerobic digestion

The changes in VFAs during anaerobic digestion are shown in Fig. 1. Total VFA (TVFA) concentrations for the control peaked at 15 d (1777 mg L^{-1}), which can be explained by the further bioconversion of rumen contents (Fig. 1a). As expected, TVFAs initially increased with the addition of oil crop straw, and were then rapidly biodegraded by methanogens or rumen bacteria. Acetic, propionic and isobutyric acids were biodegraded faster after 5, 20–25 and 15–20 d, respectively. In contrast, butyric, valeric and isovaleric acids remained very stable within the first 20–30 d and then decreased gradually. After 30 d of anaerobic digestion, the TVFA concentrations of peanut, soybean and oilseed rape straw decreased to 112.5, 111.9 and 66.0 mg L^{-1}, respectively. Similar changes in VFAs were observed for all three types of oil crop straw.

After 5 d of anaerobic digestion, the TVFAs for the three types of oil crop straw increased dramatically to 4639–4870 mg L^{-1}; the VFAs of peanut, soybean and oilseed rape straw were all dominated by acetic and propionic acids. The net VFA yields of

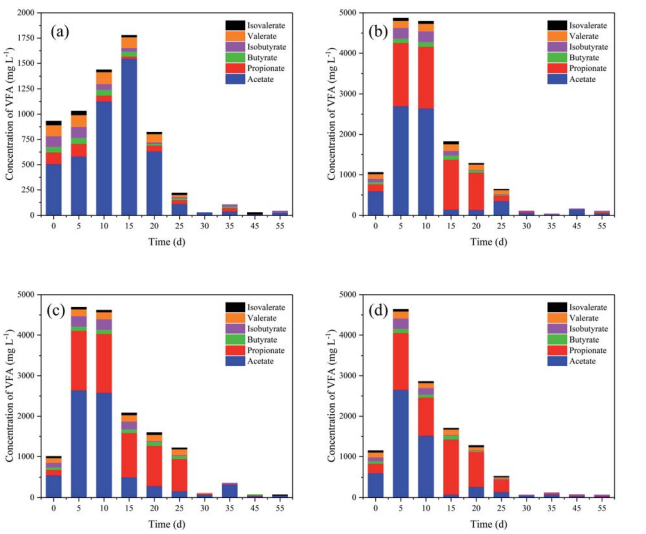

Fig. 1 Changes in volatile fatty acid (VFA) concentrations during anaerobic digestion: (a) control; (b) peanut straw; (c) soybean straw; (d) oilseed rape straw.

peanut, soybean and oilseed rape straw on day 5 reached 384.0, 366.0 and 360.8 mg g^{-1} VS, respectively. These results demonstrated that oil crop straw could be converted into VFAs *via* rumen microorganisms effectively. Rumen microorganisms are superior for the degradation of cellulosic materials compared with other microorganism inoculums, due to faster adhesion to the fibres and higher cellulolytic activities. Removing the surface substances of wax and lignin and the formation of holes by tunnelling, performed by some fungi or the protozoa *via* physical and chemical pathways, would increase the accessibility of the degradable cellulose and hemicellulose substantially.[3] Moreover, protozoa have the capability to directly swallow the lignocelluloses, and then convert lignocelluloses to polysaccharides.[28] Therefore, efficient degradation of oil crop straw by rumen microorganisms can be achieved. The powerful ability of rumen microorganisms to hydrolyse and acidify the different types of oil crop straw might provide a potential solution for preparing organic acids as industrial raw materials.

The relative abundances of individual VFA constituents (acetate, propionate, *n*- and iso-butyrate, *n*- and iso-valerate) on day 5 were further analysed, as shown in Fig. 2. Acetic, propionic and iso-butyric acids accounted for 55.2–57.5%, 35.3–37.4% and 4.0–4.2% of TVFAs, while the relative percentages of *n*-butyric (<1.3%), *n*-valeric (<1.5%) and iso-valeric acid (<1%) were very low. In the rumen system, VFAs provide 70–80% of the total energy for ruminant metabolism.[29] The relative proportions of acetic, propionic and butyric acids in this study (95.1–96.5%) were consistent with the natural rumen system (95%).[29] Propionic acid is more difficult for microorganisms to metabolise due to the slow growth rate of propionate-assimilating microbes.[30] Wang *et al.*[31] reported that elevated concentrations of propionic acid (>900 mg L^{-1}) inhibited the growth of acidogenic bacteria and methanogens. The propionate concentration in this study was as high as 1000–2000 mg L^{-1}, which would seriously inhibit the activity of methanogens, and thus of methane production (Fig. 2b). For peanut, soybean and oilseed rape straw, the total methane yields were only 116.1, 118.6 and 136.8 mL g^{-1} VS, respectively, and the net methane yields were 52.1, 54.6 and 72.7 mL g^{-1} VS, respectively, during the 55 d of digestion. The relatively high methane yield of oilseed rape straw was related to its lower lignin content, and possibly to the different carbohydrate types derived from bioconversion.

After 5 d of digestion, the pHs of peanut, soybean and rape straw all decreased to 6.70 (Fig. 2c). The opposite tendency between pH and TVFA concentration indicated that the decrease in pH was caused mainly by the VFAs. Therefore, pH can indirectly reflect the dynamic balance of VFA production–accumulation and the ability of rumen microorganisms to bioconvert straw. Following this, due to the continuous biological consumption of VFAs and the buffering effect of NH_4^+ released during anaerobic digestion, the pH increased again to 7.9–8.0. A decrease in pH (7.8) was then recorded on days 25–30, possibly due to the further degradation of some of the lignin or embedded cellulose by rumen microorganisms. Rumen microorganisms (mainly fungi) are able to degrade or decompose the rigid lignin molecular structure.[28]

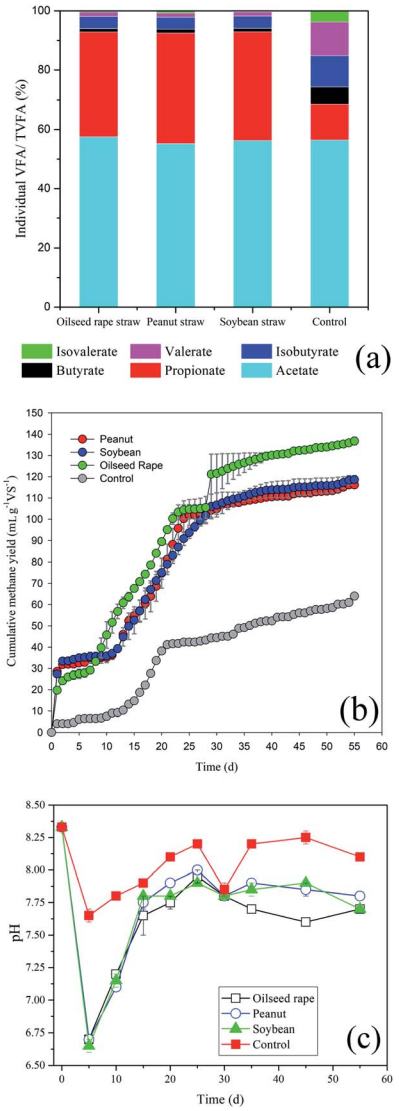

Fig. 2 (a) Distribution of individual VFAs and their proportions of total VFAs (TVFAs) for different treatments on day 5; (b) methane production during anaerobic digestion of oil crop straw inoculated with rumen fluid; (c) changes in pH during anaerobic digestion of oil crop straw.

Fluorescence spectra – parallel factor components of DOM

Fluorescence EEM spectra were used to characterize the DOM (D_0, D_5, D_{25} and D_{55} samples). The fluorescence intensities of the three peaks observed in all DOM samples changed dramatically during anaerobic digestion (see Fig. S3 of the ESI†). The total fluorescence intensity increased rapidly during the initial 5 d and then decreased gradually. The final total fluorescence intensities of the DOM (D_{55}) were significantly lower than the initial fluorescence intensities (D_0) in all treatments.

PARAFAC models with 3–10 components were computed, and the correct number of components in the data set was validated using core consistency diagnostics followed by a split-half analysis. By using PARAFAC modelling, three effective components were identified within the fluorescence EEM spectra, with a core consistency score of 94%, split-half

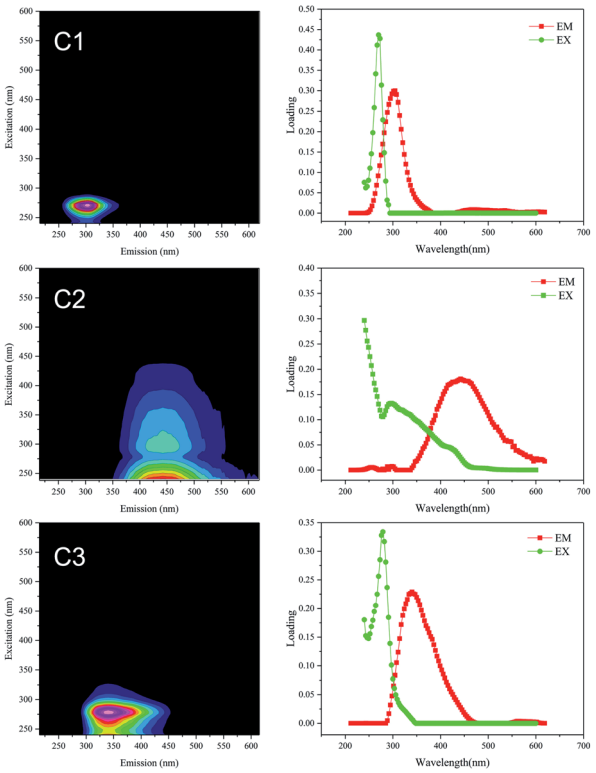

Fig. 3 Representative EEM and fluorescence spectral loading of the three components (C_1, C_2 and C_3) identified by PARAFAC analysis.

reliability of 94.4% (see Fig. S4 of the ESI†), and the model explained 98.26% of the variability in the dataset. The representative EEM and fluorescence spectral loading for the three common components (labelled C_1, C_2 and C_3) are shown in Fig. 3. Amongst these, the large spectral overlap (>120 nm) in the excitation and emission loadings of C_2 indicated a complex DOM composition.[32] The separated component spectra were examined in the online OpenFluor database[33] and identified as tyrosine-like, humic-like and tryptophan-like fluorophores, respectively, based on Tucker's congruence coefficients greater than 0.97. The sources of the fluorophores identified from the OpenFluor database closely matched those indicated by Coble's peak picking method[34] and the descriptors used for regional analysis reported by Chen *et al.*[35] (Table 2).Component 1 (C_1) located at Ex 270 nm/Em 305 nm is a tyrosine-like substance,[35] representing an amino acid-free or bound protein.[36] Component 2 (C_2), present at Ex/Em of <240/442 nm and 300/442 nm, was regarded as a humic acid species.[35] Component 3 (C_3) at Ex/Em of 279/340 nm and <240/340 nm belongs to the tryptophan-like materials[35] The protein-like fluorophores of C_1 and C_3 are typically present at lower levels than humic substances in surface waters, while the humic-like component (C_2) is one of the most frequently reported EEM-PARAFAC components in OpenFluor,[33] particularly for surface water and wastewater.

Changes in fluorescence intensity and Stokes shift of DOM during anaerobic digestion

Characterization of the EEM-PARAFAC individual components and the Stokes shift is useful for understanding the fate of DOM in the anaerobic digestion of oil crop straw. The changes in maximum fluorescence intensity (F_{max}) of the three components of the DOM during 55 d of digestion are shown in Fig. 4. Repeated-measures ANOVA indicated that the differences in the fluorescence intensities among the three different types of oil crop straw were not significant at the $P < 0.05$ level. The F_{max} values of C_1 and C_3 increased rapidly during the first 5 d of operation and then decreased gradually till day 30 (Fig. 4a and c). In the hydrolysis stage, insoluble organic polymers such as proteins were broken down to soluble derivatives such as amino acids, which increased the protein-like substances in the DOM. The changes in C_1 and C_3 implied that protein groups originating from the hydrolysis stage were broken down into non-fluorescent structures or converted to other forms, such as ammonium or carbon dioxide.[37] After 35 d of digestion, the fluorescence intensities of the C_1 and C_3 materials remained at relatively stable levels. The trends for the tyrosine-like and

Table 2 Characteristics of the three components identified by fluorescence PARAFAC modelling in this study and comparison with previously identified components

Component	Ex_{max}[a] (nm)	Em_{max}[b] (nm)	Source from OpenFluor database[33]	Description from Chen *et al.*[35]	Fluorescence peak association from references (Ex_{max}/Em_{max}) (nm/nm)	
					Coble[34]	OpenFluor database[d]
C_1	270	305	Tyrosine-like	Tyrosine-, protein-like	B: 275/305	P5: 270/310 (ref. 40) C4: 275/300 (ref. 36) C1: 275/300 (ref. 41)
C_2	<240 (300)[c]	442	Terrestrial humic-like	Soluble microbial product-like humic acid-like	M: 290–310/370–410	C1: <240/432 (ref. 42) C1: <250/440 (ref. 43) C2: 225/428 (ref. 44)
C_3	279 (<240)[c]	340	Tryptophan-like	Tryptophan-, protein-like	T: 275/340	C5: 280/340 (ref. 45) C7: 275/338 (ref. 46) C2: 279/344 (ref. 47)

[a] Maximum excitation wavelength. [b] Maximum emission wavelength. [c] Secondary fluorescence peaks in parentheses. [d] Tucker's congruence coefficient greater than 0.97.

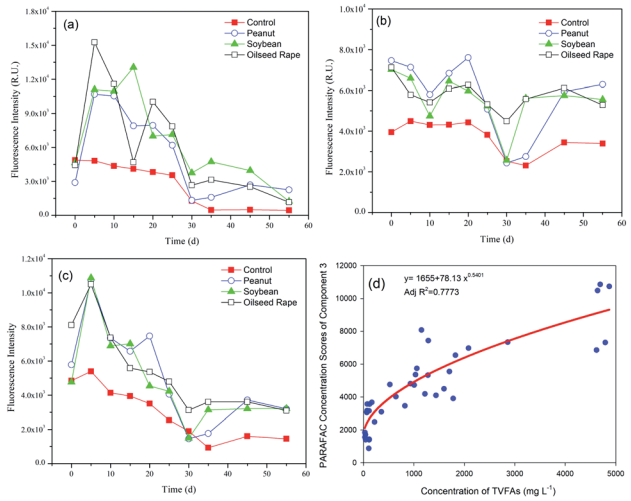

Fig. 4 Changes in the fluorescence intensity of the three components during anaerobic digestion: (a) C_1; (b) C_2; (c) C_3; (d) relationship between the fluorescence intensity of the tryptophan-like compounds and TVFA concentrations.

tryptophan-like compounds in this study were inconsistent with those reported for sewage sludge by Li *et al.*,[4] reflecting the different biodegradation mechanisms of those protein-like substances originating from different substrates.

The relationship between the intensities of the protein-like fluorescence components and the TVFA concentrations was further examined. The results showed that the fluorescence intensity of C_3 (tryptophan-like) and the concentration of TVFAs were well fitted by a power function, with Adj $R^2 = 0.7773$ (Fig. 4d). The phenomenon implied that the tryptophan-like materials were closely related to the products of hydrolysis and acidification of oil crop straw, especially the production and degradation of VFAs.

The F_{max} of C_2 generally fluctuated over time, as shown in Fig. 4b. Compared with C_1 and C_3, C_2 (humic-like materials) did not biodegrade. It is worth noting that the initial humic-like fluorescence intensity increased dramatically from 4.0×10^3 to *ca.* 7.2×10^3 RU on day 0 following the addition of different types of straw. The intensity of C_2 showed a decreasing trend in the periods 0–10 d and 20–30 d of anaerobic digestion. The humic-like substance from the anaerobic digestion of crop straw was different from that found in terrestrial ecosystems (such as forested regions and wetlands), with an Ex of <230–260 nm and an Em of 400–500 nm, which is biologically unavailable.[10] The increase in the F_{max} of C_2 in the 30–45 day period is attributed to the biodegradation of lignin and/or embedded cellulose and further formation of the humic-like substance, consistent with the pH and fluorescence intensity changes in C_1 and C_3. Previous studies have reported that lignin can be converted biologically into acid-precipitable polymeric lignin (APPL), a precursor of humic acid.[38,39] Humic-like materials are the main source of residual organic matter in the digestate of lignocellulosic biomass, which is consistent with the results found by Stephanie *et al.*[10]

Characterization of the EEM-PARAFAC individual components provides insight into the composition and fate of DOM and could be used to optimize the anaerobic digestion parameters. The accumulations of fluorescent tyrosine- and tryptophan-like substances in the DOM might become an inhibiting factor for converting substrates to biogas and might hamper the hydrolysis of insoluble particulate organic matter (POM) according to the chemical equilibrium relationship.[4] Usually, the operation of most digesters is dependent on the empirical knowledge of their operators. Monitoring EEM-PARAFAC individual components might be a useful strategy for optimizing operational parameters such as substrate concentration, C/N ratio and temperature, thereby improving the overall performance.

The distributions of the Stokes shift (measured from $Ex^{-1} - Em^{-1}$) of the DOM samples varied with anaerobic digestion time, as shown in Fig. 5. The Stokes shift reflects the loss in

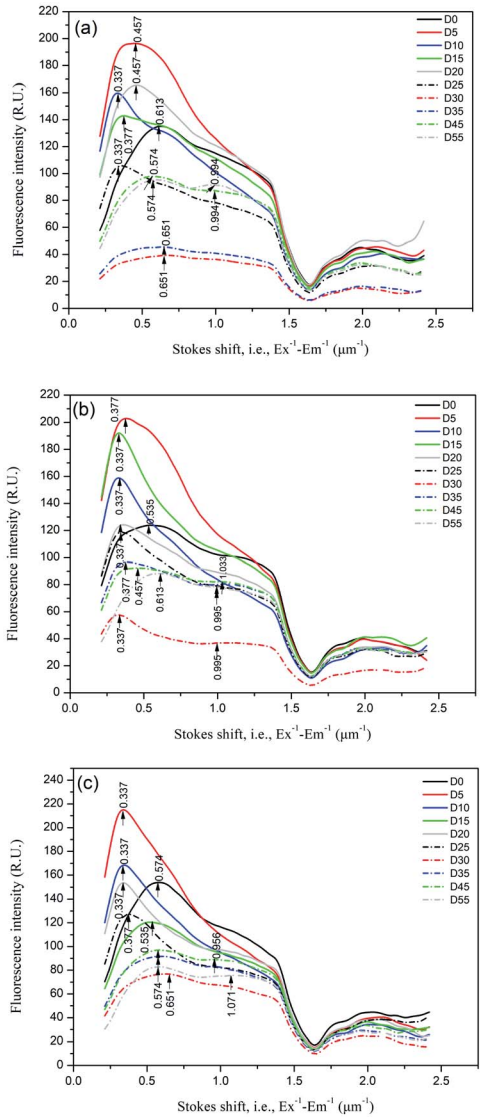

Fig. 5 Distributions of the Stokes shift (measured from $Ex^{-1} - Em^{-1}$) of the DOM samples during anaerobic digestion of oil crop straw.

relaxation energy of the fluorescence process. Xiao *et al.*[16,17] found that the Stokes shift for hydrophilic substances (HIS) was in the order < hydrophobic acids (HOA) < hydrophobic bases (HOB) due to the higher aromaticity and probably larger π-conjugated systems of the hydrophobic compared to hydrophilic fraction, according to the Lippert–Mataga equation. In this study, the changes in the Stokes shift of the fluorescence peak are readily explained by the variation in the hydrophobic/hydrophilic fraction distribution. The initial DOM samples for oil crop straw (D_0) had a distinct peak at the Stokes shift of ~0.55 μm^{-1}. After 5 d of anaerobic digestion, the fluorescence peak intensity in the smaller Stokes shift region (0.34–0.46 μm^{-1}) increased dramatically. The phenomenon might be explained by the production of hydrophilic acids (HIA) such as organic acids. Though the fluorescence signals of HIS are generally low and weak, it is believed that HIA might bear certain fluorescence characteristics due to heterozygosity or adsorption of unsaturated fragments.[15] After 45–55 d of anaerobic digestion, in addition to a weak peak at the Stokes shift of 0.46–0.65 μm^{-1}, a new weak peak at a Stokes shift of ~1.0 μm^{-1} was identified in the DOM samples. The increase in the Stokes shift of the fluorescence peak might be explained by the depletion of HIA and the biosynthesis of HOA (such as humic acid). The shape of the Stokes shift distribution curve found in this study was significantly different from that found by Xiao *et al.*,[16,17] and that is partly due to the different excitation wavelength ranges detected. It is believed that the distribution of the Stokes shift can be used to characterize the hydrophobic/hydrophilic characteristics of DOM during anaerobic digestion of crop straw, and the peak at the Stokes shift of ~1.0 μm^{-1} can be used as one of the indicators of the stabilization of anaerobic digestion.

Changes in the different fluorescence and absorbance indices

The changes in the different fluorescence and absorbance indices (humification index, A : T ratio, MFI, YFI, E_2/E_3, spectral slope ratio) were further explored. HIX is strongly correlated with DOM aromaticity and inversely correlated with carbohydrate content;[48] higher HIX values are related to the enrichment of more condensed aromatic structures and/or greater conjugation of aliphatic chains in general.[49] In this study, the DOM for all samples was derived from microbial degradation according to the measured low HIX values (<2.5). Without the addition of straw, the HIX values of the control consistently increased from 0.7 to 2.1 after 55 d of incubation (Fig. 6a), indicating that the labile organic matter in rumen liquid was further utilized by rumen microbes, which was in line with the changes in VFAs. All DOM samples exhibited the same evolutions of HIX in the presence of oil crop straw. The HIX values declined significantly due to hydrolysis, which resulted in an improvement in the bioavailability of DOM during the first 5 d. The HIX values then increased gradually to 1.53–1.65 when methanogenesis converted the dissolved intermediate products to more condensed aromatic structures, although it was still lower than that of the control. These results indicated the feasibility of using the HIX as a tool for characterizing the humification and transformation of DOM during anaerobic digestion.

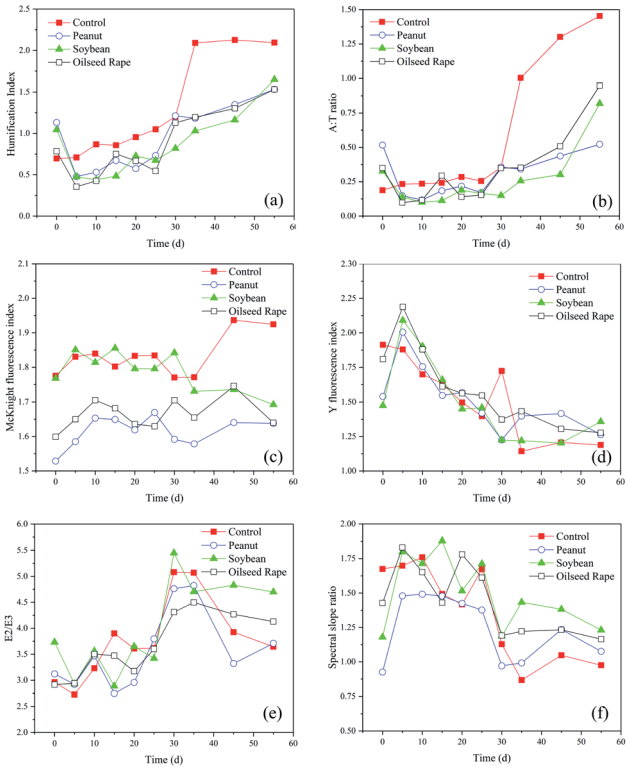

Fig. 6 Changes in the different fluorescence and absorbance indices during various stages of anaerobic digestion: (a) humification index (HIX); (b) A : T ratio; (c) McKnight fluorescence index (MFI); (d) Y fluorescence index (YFI); (e) E_2/E_3; (f) spectral slope ratio.

The relationship between HIX and individual VFA constituents was further investigated (Fig. 7a). Interestingly, propionate accumulation was always associated with low HIX values (<0.8) of the DOM. The correlations between the HIX and the F_{max} values of the three PARAFAC components were studied, and the results showed that the HIX values and F_{max} of C_1 were fitted well using a logarithmic model (Fig. 7b). The A : T ratio refers to the ratio between humic- and tryptophan-like fluorescence intensities, and can be used to describe the ratio between recalcitrant and labile fluorophores.[50] The changes in the A : T ratio in this study behaved very similarly to those of HIX (Fig. 6b). In the hydrolysis of oil crop straw, the tryptophan-like intensity increased markedly and resulted in a decrease in the A : T ratio. After 5 d of anaerobic digestion, the A : T ratios of peanut, soybean and rapeseed straw decreased from 0.52, 0.33 and 0.35 to 0.15, 0.14 and 0.10, respectively. From then on, the ratios increased gradually, which might be associated with a decrease in tyrosine-like fluorescence and a relatively stable humic-like fluorescence intensity. The A : T ratios of peanut, soybean and rapeseed straw at the end of digestion were 0.52, 0.82 and 0.95, respectively.

Two types of fluorescence indices, YFI and MFI, were adopted (Fig. 7c). The MFI values fluctuated irregularly over time during the whole digestion process. Thus, use of the MFI makes it difficult to monitor the degradation of organic matter in oil crop straw. The changes in the YFI successfully described the

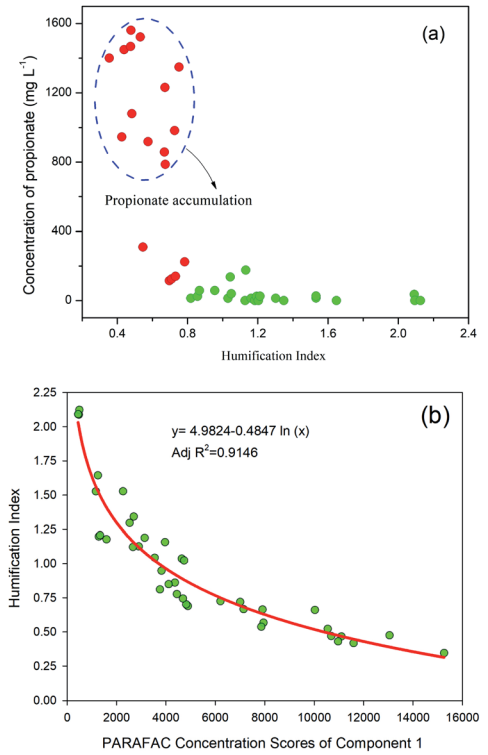

Fig. 7 Relationship between: (a) propionic acid concentration and HIX; (b) HIX and fluorescence intensity of the tyrosine-like compound.

formation of DOM by rumen microbial degradation and the humification process of newly formed DOM during anaerobic digestion (Fig. 6d). On day 5, the YFI values of peanut, soybean and rapeseed straw increased from 1.54, 1.47 and 1.81 to 2.00, 2.09 and 2.19, respectively. The YFI values then declined gradually over time and their values for peanut, soybean and rapeseed straw at the end of the process were 1.26, 1.36 and 1.28, respectively. The slight increase in YFI values on days 20–35 might be explained by the decomposition of a small amount of lignin and/or the cross-linking of hemicellulose by rumen microorganisms, which promote higher rates of lignocellulose degradation due to higher cellulolytic activities.[48] These results confirmed that, compared with MFI, YFI was better able to evaluate the anaerobic metabolic behaviours of organic matter, including protein- and humic-type substances, as also previously reported by Heo *et al.*[26]

A decreased $E_2 : E_3$ ratio typically suggested an increase in the relative sizes of molecules due to stronger light absorption by high molecular weight chromophoric DOM at longer wavelengths.[27] A steeper spectral slope (S_R) indicates lower molecular weight material with decreasing aromatic content, and a shallower (*i.e.* lower) slope suggests higher molecular weight material with increasing aromatic content. In this study, the $E_2 : E_3$ ratios increased from 2.92–3.73 to 4.31–5.44 over the period 0–30 d and decreased or remained stable over the period 30–55 d for anaerobic digestion of oil crop straw (Fig. 6e). The S_R values increased rapidly, from 0.93–1.43 (day 0) to 1.48–1.83 (day 15), and then decreased gradually to 1.08–1.23 (day 55) (Fig. 6f). This behaviour showed that the molecular size and aromatic content of the DOM first decreased and then increased throughout the entire experiment. These results were correlated with the biodegradation process of the DOM derived from the straw. First, the rumen bacteria decomposed celluloses and proteins into fermentable sugars and amino acids; these utilizable materials were then broken down further into finer structures or used to form more stable macromolecules such as humic-like materials.[51]

Correlation analysis of fluorescence indices (intensities) and absorbance indices

Correlation analysis of the various fluorescence indices (intensities) and absorbance indices was carried out by determining the Pearson correlation coefficients (R), and the results are shown in Fig. 8. These correlating indices can be used together to further describe the properties of the DOM during anaerobic digestion. As can be seen from the figure, the F_{max} of the three components modelled by EEM-PARAFAC demonstrated a strong and significant positive correlation with each other ($R > 0.6$, $P < 0.001$), especially the protein-like compounds C_1 and C_3 ($R = 0.87$). The F_{max} of the tyrosine-like (C_1) and tryptophan-like (C_3) substances correlated significantly ($P < 0.001$) and positively with YFI and S_R and correlated inversely with HIX and E_2/E_3. The F_{max} of C_2 showed a negative correlation with the E_2/E_3 ratio ($R = -0.66$, $P < 0.001$). It is expected that the relative sizes of the molecules of the DOM increased with the formation of humic-like substances. As described above, the changes in the A : T ratio behaved similarly to those of the HIX: the A : T ratio demonstrated a very strong positive correlation with the HIX ($R = 0.92$; $P < 0.001$). The YFI showed a negative correlation with HIX ($R = -0.74$; $P < 0.001$), while S_R showed negative correlations with the A : T ratio ($R = -0.67$; $P < 0.001$) and HIX ($R = -0.79$; $P < 0.001$). The more newly produced DOM (*i.e.* lower A : T ratio or HIX values) will have a lower aromatic content (*i.e.* higher S_R values) and a higher fluorescence intensity (*i.e.* higher YFI values) during anaerobic digestion (and *vice versa*).

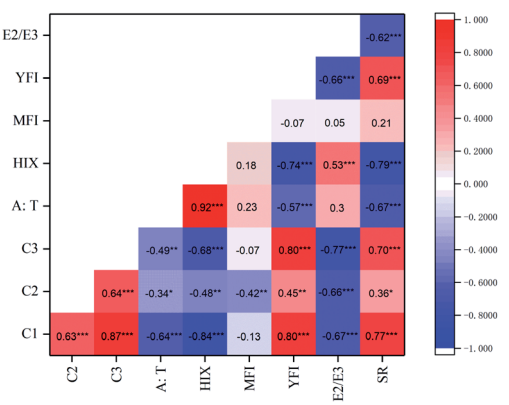

Fig. 8 Heat map of the Pearson correlation coefficients for DOM from anaerobic digestion of oil crop straw with $n = 40$ (*, ** and *** denote significance at the $P < 0.05$, $P < 0.01$ and $P < 0.001$ levels, respectively).

Conclusions

The fluorescence characteristics of DOM during 55 d of anaerobic digestion of oil crop straw inoculated with rumen liquid were investigated. The rumen microorganisms exhibited an ability to efficiently convert oil crop residue into VFAs. EEM-PARAFAC showed that three major fluorescence components, tyrosine- (C_1), humic- (C_2) and tryptophan-like substances (C_3), were identified in all of the DOM samples. The F_{max} of C_1 and C_3 increased rapidly in the first 5 d and then decreased, while C_2 did not biodegrade. The changes in the distributions of the Stokes shift of the DOM can be readily explained by the variation in the hydrophobic/hydrophilic fraction distribution. The HIX and the A : T ratio of the DOM decreased after 5 d and then increased gradually. Correlation analysis of the different fluorescence (intensities) and absorbance indices was also carried out. The EEM-PARAFAC individual components, HIX and A : T ratio can be conveniently used to characterize the degree of anaerobic conversion of organic matter, and the peak at the Stokes shift of $\sim$1.0 μm^{-1} can be used as one of the indicators of the stabilization of anaerobic digestion. These findings may assist in developing fluorescence technology for monitoring the anaerobic digestion of crop straw.

Author contributions

All of the authors contributed significantly to this research. Lianghu Su: conceptualization, investigation, methodology, writing – original draft; Mei Chen: investigation, methodology; Saier Wang: investigation; Rongting Ji: methodology; Chenwei Liu: methodology; Xueqin Lu: methodology; Guangyin Zhen: conceptualization, writing – original draft; Longjiang Zhang: conceptualization, resources, supervision.

Conflicts of interest

There are no conflicts to declare.

Acknowledgements

The authors wish to thank the Basal Research Fund of Central Public Interest Scientific Institution of Nanjing Institute of Environmental Sciences, the Ministry of Ecology and Environment (no. 2019GYZX190203 and 20160301), the Distinguished Professor in Universities of Shanghai (Oriental Scholar, no. TP2017041) and the National Natural Science Foundation of China (no. 51908380 and 51808226). The funding sources played no role in the design of the study, data collection and analysis, the decision to publish or the preparation of the manuscript.

Notes and references

1 D. Gielen, F. Boshell, D. Saygin, M. D. Bazilian, N. Wagner and R. Gorini, *Energy Strategy Reviews*, 2019, **24**, 38–50.
2 Y. R. Fang, Y. Wu and G. H. Xie, *Renewable Sustainable Energy Rev.*, 2019, **113**, 109288.
3 Z. Yue, W. Li and H. Yu, *Bioresour. Technol.*, 2013, **128**, 738–744.
4 X. Li, X. Dai, J. Takahashi, N. Li, J. Jin, L. Dai and B. Dong, *Bioresour. Technol.*, 2014, **159**, 412–420.
5 S. Shakeri Yekta, M. Gonsior, P. Schmitt-Kopplin and B. H. Svensson, *Environ. Sci. Technol.*, 2012, **46**, 12711–12719.
6 D. Lu, K. Xiao, Y. Chen, Y. N. A. Soh and Y. Zhou, *Water Res.*, 2018, **142**, 138–146.
7 R. K. Henderson, A. Baker, K. R. Murphy, A. Hambly, R. M. Stuetz and S. J. Khan, *Water Res.*, 2009, **43**, 863–881.
8 L. Yang, J. Hur and W. Zhuang, *Environ. Sci. Pollut. Res.*, 2015, **22**, 6500–6510.
9 R. Jaffé, D. McKnight, N. Maie, R. Cory, W. H. McDowell and J. L. Campbell, *J. Geophys. Res.: Biogeosci.*, 2008, **113**, G04032.
10 S. K. L. Ishii and T. H. Boyer, *Environ. Sci. Technol.*, 2012, **46**, 2006–2017.
11 K. Komatsu, T. Onodera, A. Kohzu, K. Syutsubo and A. Imai, *Water Res.*, 2020, **171**, 115459.
12 M. R. Provenzano, O. Cavallo, A. D. Malerba, C. Fabbri and C. Zaccone, *J. Cleaner Prod.*, 2018, **193**, 372–378.
13 Z. Yu, X. Liu, M. Zhao, W. Zhao, J. Liu, J. Tang, H. Liao, Z. Chen and S. Zhou, *Bioresour. Technol.*, 2019, **274**, 198–206.
14 J. Huang, L. Han and G. Huang, *Waste Manage. Res.*, 2019, **37**, 486–494.
15 J. L. Yu, K. Xiao, W. C. Xue, Y. X. Shen, J. H. Tan, S. Liang, Y. F. Wang and X. Huang, *Front. Environ. Sci. Eng.*, 2020, **14**, 31.
16 K. Xiao, B. Han, J. Sun, J. Tan, J. Yu, S. Liang, Y. Shen and X. Huang, *Environ. Sci. Technol.*, 2019, **53**, 8985–8993.
17 K. Xiao, J. Y. Sun, Y. X. Shen, S. Liang, P. Liang, X. M. Wang and X. Huang, *RSC Adv.*, 2016, **6**, 24050–24059.
18 C. Sawatdeenarunat, K. C. Surendra, D. Takara, H. Oechsner and S. K. Khanal, *Bioresour. Technol.*, 2015, **178**, 178–186.
19 L. Yang, F. Xu, X. Ge and Y. Li, *Renewable Sustainable Energy Rev.*, 2015, **44**, 824–834.
20 Z. H. Hu and H. Q. Yu, *Waste Manag.*, 2006, **26**, 1222–1228.
21 A. Quatela, A. M. Gilmore, K. E. S. Gall, M. Sandros, K. Csatorday, A. Siemiarczuk, B. B. Yang and L. Camenen, *Methods Appl. Fluoresc.*, 2018, **6**, 027002.
22 J. F. Hunt and T. Ohno, *J. Agric. Food Chem.*, 2007, **55**, 2121–2128.
23 L. Santos, A. Pinto, O. Filipe, Â. Cunha, E. B. H. Santos and A. Almeida, *PLoS One*, 2016, **11**, e0154519.
24 A. M. Hansen, T. E. C. Kraus, B. A. Pellerin, J. A. Fleck, B. D. Downing and B. A. Bergamaschi, *Limnol. Oceanogr.*, 2016, **61**, 1015–1032.
25 D. M. McKnight, E. W. Boyer, P. K. Westerhoff, P. T. Doran, T. Kulbe and D. T. Andersen, *Limnol. Oceanogr.*, 2001, **46**, 38–48.
26 J. Heo, Y. Yoon, D.-H. Kim, H. Lee, D. Lee and N. Her, *Desalin. Water Treat.*, 2016, **57**, 20270–20282.
27 J. R. Helms, A. Stubbins, J. D. Ritchie, E. C. Minor, D. J. Kieber and K. Mopper, *Limnol. Oceanogr.*, 2008, **53**, 955–969.
28 J. Liang, M. Nabi, P. Zhang, G. Zhang, Y. Cai, Q. Wang, Z. Zhou and Y. Ding, *Renewable Sustainable Energy Rev.*, 2020, **134**, 110335.

29 Basangzhuza, L. Chen, Aosiman, C. C. Yu, L. Zhao, C. S. Zhou and B. Li, *Chin. J. Anim. Nutr.*, 2017, **29**, 719–728.
30 Q. Zhang, J. He, M. Tian, Z. Mao, L. Tang, J. Zhang and H. Zhang, *Bioresour. Technol.*, 2011, **102**, 8899–8906.
31 Y. Wang, Y. Zhang, J. Wang and L. Meng, *Biomass Bioenergy*, 2009, **33**, 848–853.
32 K. R. Murphy, C. A. Stedmon, D. Graeber and R. Bro, *Anal. Methods*, 2013, **5**, 6557–6566.
33 K. R. Murphy, C. A. Stedmon, P. Wenig and R. Bro, *Anal. Methods*, 2014, **6**, 658–661.
34 P. G. Coble, *Chem. Rev.*, 2007, **107**, 402–418.
35 W. Chen, P. Westerhoff, J. A. Leenheer and K. Booksh, *Environ. Sci. Technol.*, 2003, **37**, 5701–5710.
36 P. Kowalczuk, G. H. Tilstone, M. Zabłocka, R. Röttgers and R. Thomas, *Mar. Chem.*, 2013, **157**, 170–184.
37 X. Dai, H. Yan, N. Li, J. He, Y. Ding, L. Dai and B. Dong, *Sci. Rep.*, 2016, **6**, 28193.
38 J.-J. Ko, Y. Shimizu, K. Ikeda, S.-K. Kim, C.-H. Park and S. Matsui, *Bioresour. Technol.*, 2009, **100**, 1622–1627.
39 D. L. Crawford, A. L. Pometto and R. L. Crawford, *Appl. Environ. Microbiol.*, 1983, **45**, 898–904.
40 K. R. Murphy, C. A. Stedmon, T. D. Waite and G. M. Ruiz, *Mar. Chem.*, 2008, **108**, 40–58.
41 K. R. Murphy, G. M. Ruiz, W. T. M. Dunsmuir and T. D. Waite, *Environ. Sci. Technol.*, 2006, **40**, 2357–2362.
42 L. Jørgensen, C. A. Stedmon, T. Kragh, S. Markager, M. Middelboe and M. Søndergaard, *Mar. Chem.*, 2011, **126**, 139–148.
43 C. Guéguen, C. W. Cuss, C. J. Cassels and E. C. Carmack, *J. Geophys. Res.: Oceans*, 2014, **119**, 2034–2047.
44 S. Retelletti Brogi, S.-Y. Ha, K. Kim, M. Derrien, Y. K. Lee and J. Hur, *Sci. Total Environ.*, 2018, **627**, 802–811.
45 C. L. Osburn, L. T. Handsel, M. P. Mikan, H. W. Paerl and M. T. Montgomery, *Environ. Sci. Technol.*, 2012, **46**, 8628–8636.
46 T. Lambert, S. Bouillon, F. Darchambeau, C. Morana, F. A. E. Roland, J.-P. Descy and A. V. Borges, *Biogeochemistry*, 2017, **136**, 191–211.
47 K. I. Wheeler, D. F. Levia and J. E. Hudson, *J. Geophys. Res.: Biogeosci.*, 2017, **122**, 2233–2250.
48 K. Kalbitz, J. Schmerwitz, D. Schwesig and E. Matzner, *Geoderma*, 2003, **113**, 273–291.
49 O. Martins and T. Dewes, *Bioresour. Technol.*, 1992, **42**, 103–111.
50 B. Ehnvall, Master's thesis, Swedish University of Agricultural Sciences, 2017.
51 S. Wan, B. Xi, X. Xia, M. Li, D. lv, L. Wang and C. Song, *Bioresour. Technol.*, 2012, **123**, 439–444.